Metrol. Meas. Syst., Vol. XXII (2015), No. 2, pp. 193–204.

PAN POLSKA AKADEMIA NAUK

METROLOGY AND MEASUREMENT SYSTEMS

Index 330930, ISSN 0860-8229

www.metrology.pg.gda.pl

M&MS

OPEN-PATH FTIR SPECTRAL RADIATION INTENSITY OF HOT COMBUSTION GASES – MEASUREMENT AND INTERPRETATION

Sławomir Cięszczyk

Lublin University of Technology, Institute of Electronics and Information Technology, Nadbystrzycka 38A, 20-618 Lublin, Poland
(✉ s.cieszczyk@pollub.pl, +48 81 538 4311)

Abstract

Spectral remote sensing is a very popular method in atmospheric monitoring. The paper presents an approach that involves mid-infrared spectral measurements of combustion processes. The dominant feature in this spectral range is CO_2 radiation, which is used to determine the maximum temperature of nonluminous flames. Efforts are also made to determine the temperature profile of hot CO_2, but they are limited to the laboratory conditions. The paper presents an analysis of the radiation spectrum of a non-uniform-temperature gas environment using a radiative transfer equation. Particularly important are the presented experimental measurements of various stages of the combustion process. They allow for a qualitative description of the physical phenomena involved in the process and therefore permit diagnostics. The next step is determination of a non-uniform-temperature profile based on the spectral radiation intensity with the 8 m optical path length.

Keywords: spectral remote sensing, temperature profile, hot gas, FTIR.

1. Introduction

Special techniques are required to measure the physicochemical quantities of industrial combustion processes due to difficult conditions that inhibit the access and installation of sensors [1, 2]. Spectral radiation carries a great deal of information about the combustion process. Passive mid-infrared spectral remote sensing can be applied to examine specific combustion parameters. It appears to have a great potential due to its non-intrusiveness and low complexity, which allows to place the probe in very difficult conditions (temperature, dust, vibration). It seems to be particularly suitable for continuous real-time diagnosis. In contrast to active methods, we do not have to seek an optical path between the transmitter and the detector, which is problematic in closed facilities. Generally, passive techniques cannot achieve the same accuracy as active techniques [3]; however, they offer good accuracy for temperatures in combustion processes. This method utilizes spectral radiation intensity measured along line of sight within the field of view of the spectrometer [4–6]. The measurement is very simple; however, its interpretation to determine the sought parameters remains a difficult task. The inverse problem is solved here, in a similar way to other non-invasive and indirect measurement techniques [7–11]. Absorption measurements are much easier to interpret but more difficult to perform in-situ. Furthermore, determining flame transmission spectra requires a high-intensity radiation source. Otherwise, flame self-radiation must be considered [12]. The best results in temperature measurements are achieved by passive techniques. The emission spectroscopy term [13] can be used for passive methods of measuring hot gas spectra, but it is more often used for UV–VIS and near-IR spectrometry [14].

Hot gas radiation measurements can also be used for such purposes, as comparing the characteristics of radiation emitted by flames using different fuels [15], the validation of

Article history: received on Feb. 02, 2015; accepted on May 11, 2015; available online on May 29, 2015; DOI: 10.1515/mms-2015-0027.

methods of spectral radiation modelling [16], and the verification of spectral data in databases [17]. However, difficulties in creating appropriate laboratory settings mean that such measurements can be made only in a limited number of experimental conditions.

The process of determining the sought parameters or quantities based on the measured quantity is called the inverse problem [18]. The approaches used to solve the inverse problem of spectral remote sensing can be divided into three main groups [19, 20]:

- Statistical techniques, practically not used to determine the parameters of hot gases. Their application is often limited to a linear relationship between variables.
- The forward model inversion, which is the most commonly used method. The forward simulation model calculates the measured quantity based on the sought quantities. Most inversion processes perform least squares minimization of the difference between the values of measured quantities and the values from the simulation model.
- The explicit inverse method. The method consists of finding a relationship called a mapping to convert the measured quantities to the sought ones. The most common algorithms applied for this purpose are neural networks. The training dataset can be derived from measurements or from simulation. In practice, it is very difficult to achieve a sufficient amount of measurement data; therefore, a simulation model is most often used for this purpose.

2. Mid-infrared spectral remote sensing of hot combustion gases

2.1. Classification of methods of spectral remote sensing of hot combustion gases

In the mid-infrared spectral range under consideration, radiation of particles – such as soot ones – occurs in much smaller amounts than in the near infrared spectral region. The mid-infrared region is dominated by the carbon dioxide band, which contains information about the observed path. A general feature of the 4.3 μm CO_2 spectrum is higher temperature than concentration sensitivity, and therefore much better temperature determination [21]. The methods of utilizing the spectra can be divided according to the type of temperature heterogeneity of the studied environment and the specifics of the inversion algorithm. The approaches used to determine the temperature distribution are different from those used for typical atmospheric measurements.

In general, the temperature retrieval may involve:

- Uniform temperature area [22–24].
- Determination of the maximum temperature of a nearly homogeneous area or an area of assumed homogeneity [25–27].
- Determination of the temperature profile of an axisymmetric area [28–30].
- Determination of the temperature profile of a non-uniform medium [31–33].

Inverse problem solution methods for determining the temperature can be divided as follows:

- Comparison of the highest CO_2 spectral intensity and blackbody radiation [24, 28].
- Comparison of the measured and simulated CO_2 spectra using iterative least square methods [34–36].
- Use of a neural network trained with synthetic spectra (forward problem) [28–30].

The determined temperature can belong to one of the following ranges:

- Plume or stack exhaust temperatures, typically below 600 K [24, 25, 37].
- Hot exhaust gases, with temperatures between 500 K and 1000 K [28, 29, 34].
- Flame temperatures above 1000 K [38, 39].
- Very high flame temperatures up to 5000 K [40, 41].

2.2. Critical analysis and brief review of methods

For a typical remote sensing resolution (0.5–5 cm^{-1}), the whole 2000–2400 cm^{-1} CO_2 range is required for inversion purposes. A very high resolution allows using the narrow spectral range between 2379 and 2397 cm^{-1} [34]. However, even then, the procedure of downgrading the resolution from 0.02 cm^{-1} to 25 cm^{-1} is considered to be more reliable with the least square spectra adjustment [42].

In the case of smoke stack plume monitoring, the temperature can be remotely estimated by comparing the CO_2 maximum spectral intensity with black-body radiance. Next, the estimated value is used to calculate the concentration of different molecules by trial and error [43]. A slightly different approach to plume temperature remote sensing involves using the intensity ratio of CO_2 at widely separated wavelengths of 4.19668 and 14.5023 μm, independent of gas concentration [37]. Absolute radiation intensity measurement spectra expressed in radiometrical units (radiance) are required for most inversion techniques. Inaccuracy in the radiometric calibration can cause additional errors in the subsequent parameter retrieval process [44]. The ratio method eliminates errors caused by inaccuracies in the absolute spectral radiance measurement. However, some error can still result from spectrometer spectral responsivity, particularly if the chosen intensities are widely separated in wavelengths. Intensities lying close to each other are less prone to the relative pattern inaccuracies of the measuring instrument spectra.

The most commonly used hot gas inversion algorithm involves iterative procedures even to determine the properties of a homogeneous layer [23]. Multiple line emission in bands specified by 3 filters is used for an average temperature, H_2O and CO_2 concentrations estimation from the radiance of the combustion flow [23]. The temperature can be estimated directly by comparing the 2350 cm^{-1} CO_2 radiance intensity with the Planck curve for a short uniform optical path and optically thick conditions [24]. A similar principle is used for the 14 m path in a coal-fired boiler [27] and 1.3 MW pulverized coal flame [25]. The gas temperature is retrieved by a least-squares optimization method comparing the 4.6 μm CO_2 emission region (furnace CO_2 region) with blackbody radiance. The uniform temperature, isotropic scattering and 14 % gas concentration are assumed.

CO_2 radiation is also used for the temperature calculation in a flow cuvette [45]. It is assumed that cold CO_2 absorption does not influence the strong 2270 cm^{-1} emission intensity. In some cases, atmospheric correction (reduction of a strong spectral feature of cold CO_2) is applied to obtain clear emission spectra [46]. Another example is the use of CO_2 radiance at 2078 cm^{-1} for the remote mapping of stack plume structure contours from the 595 m distance [26].

Regularization methods are proposed to increase the stability and convergence of iterative solution methods for different types of the inverse problem [47, 48]. The retrieved temperature profile can be provided in a parametric form. One very interesting approach is a base function-based inversion method, which uses a set of functions to present the searched temperature distribution [33, 36]. Another regularization technique uses appropriate limitation assumptions regarding the values of the desired physical quantities. Additional knowledge about the studied phenomenon based on considering the physical constraints of the temperature profile significantly increases accuracy of the inversion procedure. The best results are achieved using adequate assumptions about the considered profile [39].

Neural network inverse models are alternatives to physical iterative methods. Neural networks are often used to determine atmospheric parameters based on spectral radiation. In the case of combustion processes, the problem of non-linearity is increased due to much higher temperatures under consideration. Another important difference is higher ranges of changes in the sought parameters, as well as worse a priori knowledge. The use of neural networks to determine the temperature of a plume based on radiation in the considered spectral range has

also been proposed [28–30]. Tests were made for high spectral resolution simulation data accompanied by PCA dimensionality reduction. The retrieved profile was divided into five equal parts [28] or was limited to axial symmetry [29].

It should be noted that the above presented methods do not always relate to determination of physical quantities based on spectrum measurements, but are often only verification of spectrum modelling. The temperature, in diagnostics of industrial processes, is instead determined by assuming a homogenous environment and employing a method of comparing the CO_2 spectral radiation intensity with the black body spectrum. For exhaust gases, the assumption concerns axial symmetry. In other cases, the analysis concerns conditions produced in the laboratory, generally characterized by a higher level of considerations and mathematically more advanced inversion methods. However, not all the proposed methods can be directly applied to real industrial process measurements. The main limitations are simplifying assumptions relating to the laboratory study that cannot be easily adapted in practice.

3. Hot gas emission spectrum modelling

Hot gas spectral radiation intensity modelling of homogenous or nonhomogeneous profiles is an important problem in spectral remote sensing. Modelling a variety of possible cases can help fully understand the considered phenomenon and better cope with real object measurements, which is a very important step in the cognitive process of metrology [49]. It is also necessary for calculation of the synthetic data used to build an inverse model linking the measurement and sought quantities (explicit inverse), as well as in the forward model iterative inversion.

To accurately model the spectral radiation intensity, an appropriate spectral database is necessary. Many works have been devoted to the measurement of gas spectra at high temperatures and their comparison with currently available spectral databases. This research ensures that simulation spectra data are reliable. The importance of such works lies in the fact that it is very difficult to build an adequate test stand. To test the quality of spectral data with a specified precision, it is necessary to produce an observed path with uniform temperature and gas concentration. For this purpose, a heated gas cell for hot gas analysis in temperatures up to 1373 K was developed and tested for the CO_2 gas [50]. Another heated cell with the temperature deviation of less than 1% along the 38 cm path was developed [51]. Another research uses a hot gas cell with the 53,3 cm length to verify spectral gas models with experimental measurements [52]. The study shows that the HITEMP2010 line-by-line model and the RADCAL and EM2C statistical narrow-band models present a very good agreement with experimental results. Low-resolution calculation by the weighted sum of grey gases model (WSGGM) is also proposed for the temperature inversion based on CO_2 radiation.

The equation of radiative energy transfer accounts for the temperature heterogeneity of the observed path. The radiation intensity for a given wavelength can be written as follows:

$$I_\lambda(0) = -\int_0^L L_\lambda(T(l))\frac{\partial \tau_\lambda(l)}{\partial l}dl, \tag{1}$$

where $T(l)$ – the temperature distribution along the observed path, $\tau_\lambda(l)$ – the transmissivity between spectrometer ($l = 0$) to the end of analysed path ($l = L$), $L_\lambda(T)$ – the black body radiance at the temperature T.

The radiative transfer equation can also include a scattering term, which may significantly affect the calculated transmissivity [53, 54]. For the combustion of biomass gasification gases in the mid-infrared spectral range, it can be assumed that scattering can be neglected. To compare the modelled and measured spectra convolution with the spectrometer ILS

(instrumental line shape) is also needed. Exemplary simulation spectra (HITEMP [55] modelling) for profiles with different path lengths are presented in Fig. 1.

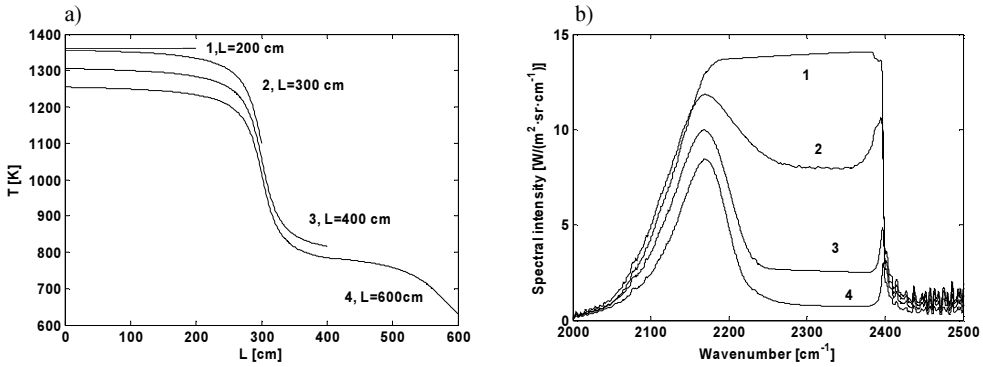

Fig. 1. Exemplary temperature profiles and corresponding spectra of CO_2 (10% CO_2, 1 cm^{-1} resolution).

4. Measurement of spectral radiation with OP-FTIR spectrometer

A Bruker FTIR (Fourier Transform Infrared Spectrometer) OPAG−33 was used for the spectral radiation measurement. All spectra were acquired with 1 cm^{-1} resolution. The measurements were performed on a test stand used to study the combustion phenomena of gases from gasification processes [56]. The power of the test stand was 1.5 MW, and its length was approximately 8 m. Measurements were made on two sides, one facing the flame and the other – the exhaust gases (Fig. 2). The measuring path consisted of multiple parts: the hottest flame part, followed by the region of rapidly cooling exhaust gases, followed by the slow cooling of the exhaust gases. The spectrometer was located approximately 3 m from the end of the test stand. The diaphragm system was used to limit the detector signal to avoid nonlinearities.

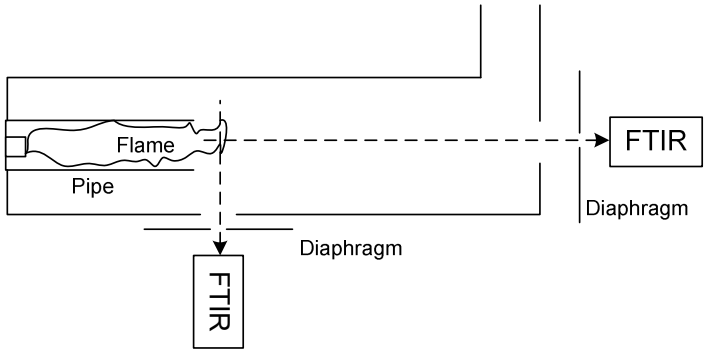

Fig. 2. A diagram of measurement setup and performed experiment.

Figure 3 shows the spectra of gases from the gasification process flowing through the combustion chamber to the chimney. These spectra can be observed from the side when there is no combustion. A strong background radiation from heated parts of the combustion chamber can be observed. Fig. 3a shows the whole measured spectral range. Fig. 3b presents spectra in the range limited to interesting spectral emission characteristics of carbon monoxide and carbon dioxide. Two curves measured at 30-second intervals can be observed. The spectrum labelled 3b2 (Fig. 3b) is of a lower intensity than 3b1 due to a lower temperature of heated element of

the observed combustion chamber and a lower temperature of gases flowing from the gasification process.

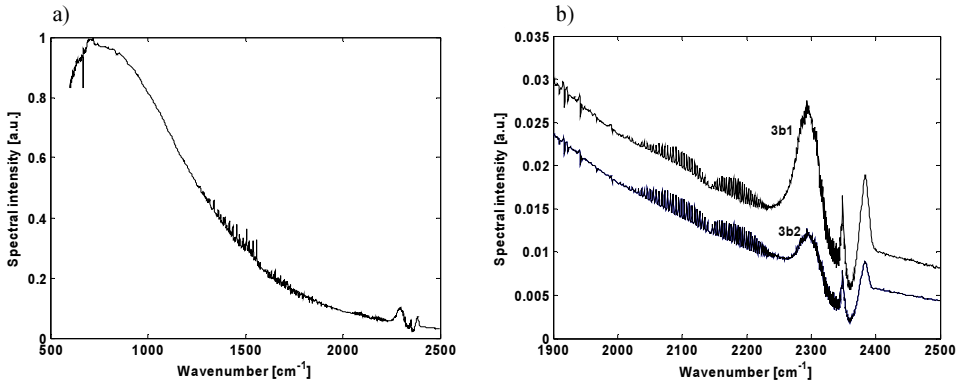

Fig. 3. The spectra of gases flowing from the gasification process to the chimney through the combustion chamber.

Figure 4 shows the spectrum of flame as observed from the side. The gases were ignited by an additional gas burner. The firing up process was accompanied by an increase in the intensity of radiation (Fig. 4b). The spectrum labelled 4b1 (Fig. 4b) is measured after ignition, the spectrum 4b2 represents the intermediate firing up process, and 4b3 – the stable combustion. A difficulty in access to controlling the process and a necessity of avoiding saturation of a detector cause that the spectra intensity is not measured in radiometric quantity. However, the spectrum pattern, as well as the relative intensity between particular spectra are preserved. The whole spectrum (Fig. 4a) is dominated by the strongest CO_2 intensity within wavenumbers 2200–2300 cm^{-1}. It creates a characteristic peak with additional absorption from the colder parts (2300–2380 cm^{-1}), primarily related to the atmospheric air between the flame and the spectrometer. During the initial phase of the gasification process, the level of produced gases supplying the burner is changing, causing instability and large fluctuations of the flame radiation intensity. During normal operation, the rate of flowing gases is nearly constant, so the flame radiation intensity changes only to a small extent.

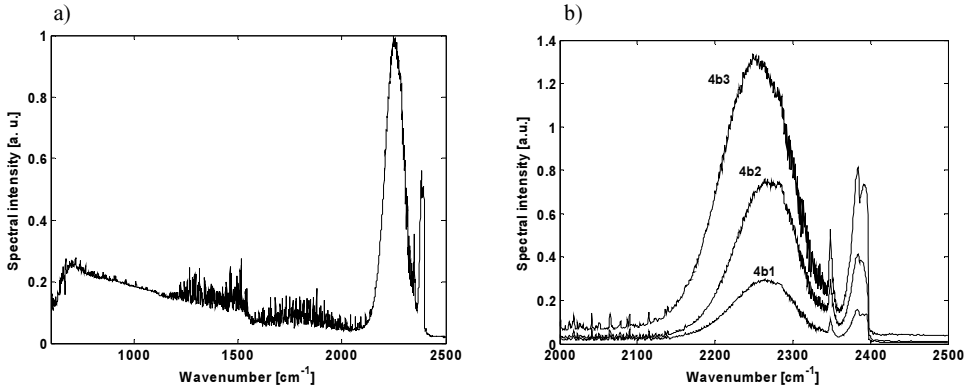

Fig. 4. The spectrum of the combustion process when viewing the side of the flame during the initial phase of combustion.

In Fig. 5a, the spectrum of the additional small gas burner used to fire the main burner is presented. The path between the flame and the spectrometer is approximately 10 meters, causing total absorption in the 2300–2380 cm^{-1} range by the cold CO_2 in the combustion chamber and the ambient air between the chamber and the spectrometer. The combustion chamber does not contain gases from the gasification process. Fig. 5b shows the spectra of the initial process of combustion. A significant increase in the flame intensity occurs, as represented by CO_2 spectral features of 5b1 and 5b2 spectra. Absorption characteristics of colder gas (CO rotational lines in 2050–2240 cm^{-1} and CO_2 in 2250–2380 cm^{-1} range) in the chamber are shown in contrast with CO_2 flame emission characteristics. Particularly noticeable are the rotational lines of CO that is not converted to CO_2 due to the low combustion temperature. After the initial combustion process, the conversion of CO to CO_2 is much more efficient because of a higher combustion temperature (6a1 in Fig. 6a and 6b1 in Fig. 6b). Thus, the exhaust gases in the combustion chamber outside the flame are essentially hotter (mainly CO_2), which is manifested in the absorption characteristics compared with the hottest flame region. The absorption spectrum of CO against the hot flame CO_2 observed in the initial stage of the process is much less visible.

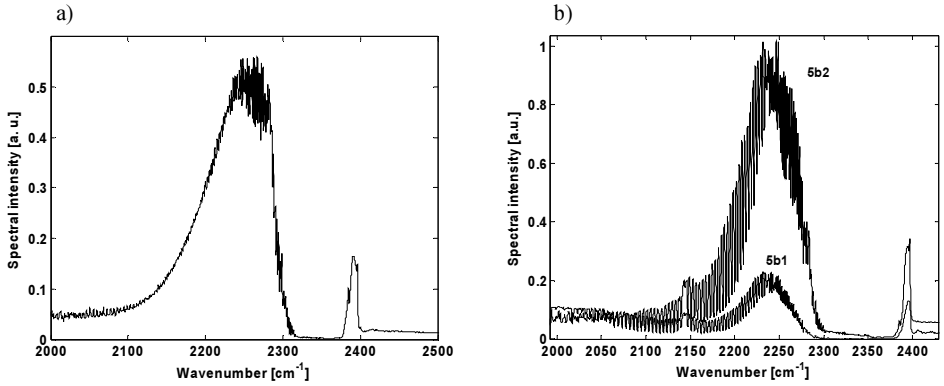

Fig. 5. The spectra of the additional gas burner used to ignite the main burner (a) and the spectra of gases during the initial stage of combustion process taken from the exhaust outlet (b).

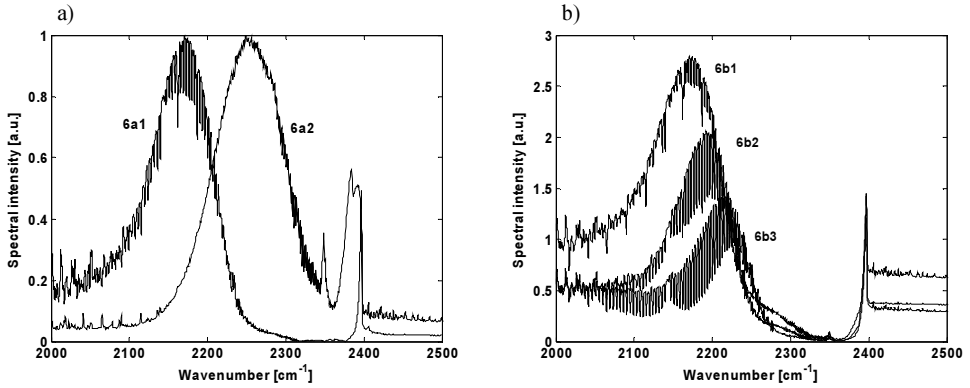

Fig. 6. Comparison of the spectra from the side and back of flame (a); the final stage of combustion process and quenching the flame observed from the back of the flame (b).

In Fig. 6a, the normalized spectra measured from the side (6a1) and back (6a2) of the combustion chamber were compared. The emission spectrum from the side is narrower (2120–2400 cm^{-1}) due to a lower value of the product of CO_2 concentration and path length. The absorption features (2300–2380 cm^{-1}) are also narrower because they come from atmospheric air between the chamber and spectrometer. For the measurement of the back of the chamber, the absorption in the 2180–2300 cm^{-1} range comes from hot exhaust gases in the combustion chamber outside the flame.

Figure 6b shows the process of expiring the flame represented by measurements referred as 6b1, 6b2 and 6b3. The decreasing concentration of combustible gases from the gasification process decreases the flame temperature, which reduces the radiation intensity in the 2100–2250 cm^{-1} region and leads to the worst conversion of CO to CO_2. The latter phenomenon is observed in the appearance of the CO rotational line structure against the continuous background and CO_2 radiation emission.

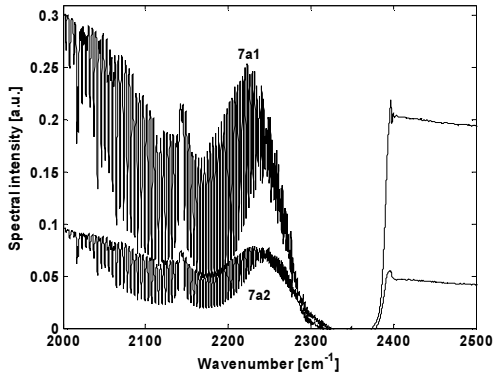

Fig. 7. The spectra of gases flowing from the gasification process after extinguishing the flame, measured from the back of combustion chamber.

Figure 7 shows the absorption spectrum of gases from the gasification process flowing through the combustion chamber after extinguishing the flame. The spectrum is observed against the continuous background of burner parts heated to a high temperature. These elements are cooled, so that lowering the continuous intensity between 7a1 and 7a2 spectra can be observed.

Methods that consist in the interpretation of CO_2 spectra use the spectral radiation intensity for each wavenumber directly. In the simplest method, optically thick conditions are assumed, and only the maximum temperature of the observed path is derived. A calibration procedure is required for this radiance spectrum interpretation, so that the measured spectrum is presented in radiance units ($W/(cm^2 \cdot sr \cdot cm^{-1})$). However, if the radiation gas cloud occupies only a fraction f of the spectrometer field of view, the acquired radiance L_s will be only part of the emitted intensity L:

$$L_s = f \cdot L. \tag{2}$$

The presented emission spectra are not measured in absolute units of spectral radiance, so they represent only a spectral pattern, not the spectral intensity, due to a difficult access to the process and a need to reduce the high flame radiation intensity by the diaphragm system. Hence, the spectrum (Fig. 8b) is normalized to unity.

The inversion procedure used for the temperature inversion (Fig. 8a) is based on matching the subsequent parts of the spectrum. Knowledge of the flame length allowed adjustment of the

temperature profile as an *arctan(l)* function. The maximum temperature of the flame and the end of the transition flame zone (2–4 m) were modelled. This part corresponds to comparison of the spectrum in the 2100–2200 cm^{-1} range. Another *arctan(l)* function represents the part of the profile farther from the flame, in which the exhaust gases are colder. This part corresponds to the spectrum in the 2200–2250 cm^{-1} range. The remaining part of the spectrum in the 2250–2400 cm^{-1} range is related to atmospheric CO_2 between the tested object and the spectrometer.

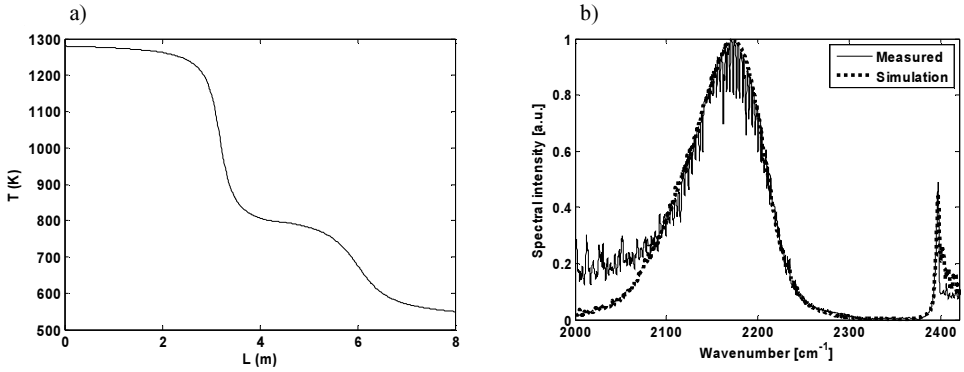

Fig. 8. The retrieved temperature profile (a), comparison of the measurement and simulation spectra (b).

5. Conclusions

This paper presents a study of mid-infrared spectral remote sensing methods used for monitoring combustion processes. The first part of the analysis covers methods of spectrum measurement and their interpretations for various processes, as described in the literature. The approaches can be divided into laboratory-scale and industrial investigation of objects. The latter can be divided into measurements of exhaust gases from engines and turbines and measurements in closed objects (boilers, furnaces). Literature reports regarding spectra inside facilities are very rare, and their interpretation is based on the assumption that CO_2 radiates as strongly as the black body. More advanced inversion methods are used for laboratory environments. These techniques, however, require additional information regarding the gas concentration, the type of tested heterogeneity of the considered profile or its axial symmetry. Laboratory conditions allow also measurements with a higher spectral resolution.

The experimental part of the paper addresses spectrum measurements of the combustion of gases from biomass gasification processes. The spectra contain important information about the state of the occurring process. The dominant spectral feature is, of course, the spectrum of CO_2 in the 2100–2400 cm^{-1} range. The gases produced during the gasification process contain a very high CO content, so its rotational lines are also visible in the acquired spectra. Interesting phenomena can be observed, especially in the ignition and extinguishing phases of the combustion process. In both these phases there is an increase in CO, and therefore its spectral features appear in the spectrum. This phenomenon is accompanied by a decreased intensity of CO_2 radiation, indicating a reduction of the process temperature. Comparing the emission spectra of long and short measurement paths (rear and side of the flame) highlights an impact of measuring distances on the observed spectral characteristics of CO_2. Finally, the quantitative analysis of the measured spectrum is presented. The algorithm used here consists in matching of the subsequent fragments of the investigated spectrum. The determined temperature profile is presented in the form of a composition of two *arctan(l)* functions. This profile representation results from the qualitative analysis of the object and the measured spectrum.

References

[1] Docquier, N., Candel, S. (2002). Combustion control and sensors: a review. *Progress in Energy and Combustion Science*, 28(2), 107–150.

[2] Ballester, J., Garcia-Armingol, T. (2010). Diagnostic techniques for the monitoring and control of practical flames. *Progress in Energy and Combustion Science*, 36(4), 375–411.

[3] Schafer, K., Brockmann, K., Heland, J., Wiesen, P., Jahn, C., Legras, O. (2005). Multipass open-path Fourier-transform infrared measurements for nonintrusive monitoring of gas turbine exhaust composition. *Applied Optics*, 44(11), 2189–2201.

[4] Koehler, F., Small, G., Combs, R., Knapp, R., Kroutill, R. (2001). Automated detection of sulphur dioxide in stack emissions by passive Fourier transform infrared spectrometry. *Vibrational Spectroscopy*, 27(2), 97–107.

[5] Wan, B., Small, G.W. (2008). Airborne passive Fourier transform infrared remote sensing of methanol vapour from industrial emissions. *The Analyst*, 133, 1776–1784.

[6] Sulub Y., Small, G.W. (2007). Quantitative determination of ethanol in heated plumes by passive Fourier transform infrared remote sensing measurements. *The Analyst*, 132, 330–337.

[7] Mroczka, J., Szczuczyński, D. (2013). Improved technique of retrieving particle size distribution form angular scattering measurements. *J. Quant. Spectrosc. Radiat Transf.*, 129, 48–59.

[8] Ravi, J., Lu, Y., Longuemart, S., Paoloni, S., Pfeiffer, S., Thoen, J., Glorieux, C. (2005). Optothermal depth profiling by neural network infrared radiometry signal recognition. *Journal of Applied Physics*, 97, 014701.

[9] Pastorino, M. (2004). Recent inversion procedures for microwave imaging in biomedical, subsurface detection and non-destructive evaluation applications. *Measurement*, 36, 257–269.

[10] Świrniak, G., Głomb, G, Mroczka, J. (2014). Inverse analysis of the rainbow for the case of low-coherent incydent light to determine the diameter of a glass fiber. *Applied Optics*, 53(19), 4239–4247.

[11] Świrniak, G., Głomb, G., Mroczka, J. (2014). Inverse analysis of light scattered at a small angle for characterization of a transparent dielectric fiber. *Applied Optics*, 53(28), 7103–7111.

[12] Egorov, O., Voitsekhovskaya, O., Kashirskiia, D., Tsvykc, R., Sazanovichc, V., Sherstobitovc, M. (2014). The optical method for determining the thermodynamic parameters of hot gases. *J. Quant. Spectrosc. Radiat Transf.*, 147, 38–46.

[13] Bourayou, R., Vaillon, R., Sacadura, J.F. (2002). FTIR low resolution emission spectrometry of a laboratory-scale diffusion flame: experimental set-up. *Experimental Thermal and Fluid Science*, 26, 181–187.

[14] Parameswaran, T., Hughes, R., Gogolek, P., Hughes, P. (2014). Gasification temperature measurement with flame emission spectroscopy. *Fuel*, 134, 579–587.

[15] Boulet, P., Parent, G., Acem, Z., Collin, A., Sero-Guillaume, O. (2011). On the emission of radiation by flames and corresponding absorption. *Fire Safety Journal*, 46, 21–26.

[16] Nam, H.J. Kwon, O.J. (2014). Infrared radiation modeling of NO, OH, CO, H2O and CO2 for emissivity/radiance prediction at high temperature. *Infrared Physics & Technology*, 67, 283–291.

[17] Fleckl, T., Jager, H., Obernberger, I. (2002). Experimental verification of gas spectra calculated for high temperatures using the HITRAN/HITEMP database. *J. Phys. D: Appl. Phys.*, 38, 3138–3144.

[18] Mroczka, J., Szczuczyński, D. (2009). Inverse problems formulated in terms of first-kind Fredholm integral equations in indirect measurement. *Metrol. Meas. Syst.*, 16(3), 333–357.

[19] Sharkov, E.A. (2003). *Passive Microwave Remote Sensing of the Earth*, Springer Verlag, Berlin, 526–530.

[20] Krasnopolsky, V.M., Schiller, H. (2003). Some neural network applications in environmental sciences. Part I: forward and inverse problems in geophysical remote measurements. *Neural Networks*, 16, 321–334.

[21] Ren, T., Modest, M. F., Fateev, A., Clausen, S. (2015). An inverse radiation model for optical determination of temperature and species concentration: Development and validation. *J. Quant. Spectrosc. Radiat Transf.*, 151, 198–209.

[22] Lim, J., Sivathanu, Y., Ji, J., Gore, J. (2004). Estimating scalars from spectral radiation measurements in a homogeneous hot gas layer. *Combustion and Flame*, 137, 222–229.

[23] Spelman, J., Parker, T.E., Carter, C.D. (2003). Fiber-coupled multiple-line emission measurements to determine temperature, CO2, and H2O. *J. Quant. Spectrosc. Radiat Transf.*, 76, 309–330.

[24] Bak, J., Clausen, S. (2002). FTIR emission spectroscopy methods and procedures for real time quantitative gas analysis in industrial environments. *Measurement Science and Technology*, 13, 150–156.

[25] Clausen, S. (1995). Infrared combustion diagnostics in fluctuating flames. *Proc. of SPIE*, 2506, 30–44.

[26] Gross, K.C., Bradley, K.C., Perram, G.P. (2010). Remote Identification and quantification of Industrial Smokestack Effluents via Imaging Fourier-Transform Spectroscopy. *Environmental Science & Technology,* 44, 9390–9397.

[27] Rego-Barcena, S., Saari, R., Mani, R., El-Batroukh, S., Thomson, M.J. (2007). Real time, non-intrusive measurement of particle emissivity and gas temperature in coal-fired power plants. *Measurement Science and Technology*, 18, 3479–3488.

[28] Garcia-Cuesta, E., Galvan, I. M., de Castro, A.J. (2008). Multilayer perceptron as an inverse model in a ground-based remote sensing temperature retrieval problem. *Engineering Application of Artificial Intelligence*, 21, 26–34.

[29] Garcia-Cuesta, E., de Castro, A.J., Galvan, I.M., Lopez, F. (2014). Temperature Profile Retrieval in Axisymmetric Combustion Plumes Using Multilayer Perceptron Modeling and Spectral Feature Selection in the Infrared CO2 Emission Band. *Applied Spectroscopy*, 68(8), 900–908.

[30] Cięszczyk S. (2014). Non-Luminous Flame Temperature Determination Method Based on CO2 Radiation Intensity. *Acta Physica Polonica A*, 126(6), 1235–1240.

[31] Vitkin, E., Zhdanovich, O., Tamanovich, V., Senchenko, V., Dozhdikov, V., Ignatiev, M., Smurov I. (2002). Determination of the temperature and concentration for the products of combustion of hydrocarbon fuel on the basis of their infrared self-radiation. *International Journal of Heat and Mass Transfer*, 45, 1983–1999.

[32] Kim, H.K., Song, T.H. (2002). Measurement of gas temperature distributions in a test furnace using spectral remote sensing. *J. Quant. Spectrosc. Radiat Transf*., 73, 517–528.

[33] Kim, H.K., Song, T.H. (2004). Characteristics of SRS inversion for measurement of temperature and CO2 concentration profile of a combustion gas layer. *J. Quant. Spectrosc. Radiat Transf.*, 86, 181–199.

[34] Al Khoury, P., Chavent, G., Clements, F., Herve, P. (2005). Inversion of spectroscopic data, application on CO2 radiation of flame combustion. *Inverse Problems in Science and Engineering*, 13(3), 219–240.

[35] Song, T.H. (2008). Spectral Remote Sensing for Furnaces and Flames. *Heat Transfer Engineering*, 29(4), 417–428.

[36] Kim, H.K., Song, T.H. (2005). Determination of the gas temperature profile in a large-scale furnace using a fast/efficient inversion scheme for the SRS technique. *J. Quant. Spectrosc. Radiat Transf.*, 93, 369–381.

[37] Jellison, G.P., Miller, D.P. (2006). Determination of gas plume temperature from molecular emission spectra. *Optical Engineering*, 45(1), 016201–1–8.

[38] Ko, J.Y., Kim, H.K., Song, T.H. (2009). Inversion of combustion gas temperature/concentration profile with radiation/turbulence interaction using SRS. *J. Quant. Spectrosc. Radiat Transf.*, 110, 1199–1206.

[39] Woo, S.W., Song, T.H. (2002). Measurement of gas temperature profile using spectral intensity from CO_2 4,3um band. *International Journal of Thermal Sciences*, 41, 883–890.

[40] Depraz S., Perrin M.Y., Soufiani A. (2012). Infrared emission spectroscopy of CO_2 at high temperature. Part I: Experimental setup and source characterization, *J. Quant. Spectrosc. Radiat Transf*., 113, 1–13.

[41] Depraz, S., Perrin, M.Y., Soufiani, A. (2012). Infrared emission spectroscopy of CO2 at high temperature. Part II: Experimental results and comparisons with spectroscopic databases, *J. Quant. Spectrosc. Radiat Transf*., 113, 14–25.

[42] Soufiani, A., Martin, J., Rolon, J., Brenez L. (2002) Sensitivity of temperature and concentration measurements in hot gases from FTIR emission spectroscopy. *J. Quant. Spectrosc. Radiat Transf*., 73, 317–327.

[43] Hilton, M., Lettington, A.H., Mills, I.M. (1995). Quantitative analysis of remote gas temperatures and concentrations from their infrared emission spectra. *Measurement Science and Technology*, 6, 1236–1241.

[44] Tank, V. (1999). Spectrometric hot gas remote sensing – investigations on calibration errors. *Journal of Molecular Structure*, 482–483, 545–550.

[45] Grosch, H., Fateev, A., Nielsen, K.L., Clausen, S. (2013). Hot gas flow cell for optical measurements on reactive gases. *J. Quant. Spectrosc. Radiat Transf.*, 130, 392–399.

[46] Harley, J.L., Rankin, B.A., Blunck, D.L., Gore, J.P., Gross, K.C. (2014). Imaging Fourier-transform spectrometer measurements of a turbulent nonpremixed jet flame. *Optics Letters*, 39(8), 2350–2353.

[47] Mroczka, J., Szczuczyński, D. (2010). Improved regularized solution of the inverse problem in turbidimetric measurements. *Applied Optics*, 49(24), 4591–4603.

[48] Mroczka, J., Szczuczyński, D. (2012). Simulation research on improved regularized solution of inverse problem in spectral extinction measurements. *Applied Optics*, 51(11), 1715–1723.

[49] Mroczka, J. (2013). The cognitive process in metrology. *Measurement*, 46, 2896–2907.

[50] Clausen, S., Bak, J. (2002). A hot gas facility for high-temperature spectrometry. *Measurement Sciences and Technology*, 13, 1223–1229.

[51] Evseev, V., Fateev, A., Clausen, S. (2010). High-resolution transmission measurements of CO_2 at high temperatures for industrial applications. *J. Quant. Spectrosc. Radiat Transf*, 113, 222–2233.

[52] Becher, V., Clausen, S., Fateev, A., Spliethoff, H. (2011). Validation of spectral gas radiation models under oxyfuel conditions. Part A: Gas cell experiments. *International Journal of Greenhouse Gas Control*, 5S, S76–S99.

[53] Czerwiński, M., Mroczka, J., Girasole, T., Gouesbet, G., Grehan, G. (2001). Light-Transmittance Predictions Under Multiple-Light-Scattering Conditions. I. Direct Problem: hybrid-Method Approximation. *Applied Optics*, 40(9), 1514–1524.

[54] Czerwiński, M., Mroczka, J., Girasole, T., Gouesbet, G., Grehan, G. (2001). Light-Transmittance Predictions Under Multiple-Light-Scattering Conditions. II. Inverse Problem: Particle Size Determination. *Applied Optics*, 40(9), 1525–1531.

[55] Rothman, L.S., Gordon, I.E., Barber, R.J., Dothe, H., Gamache, R.R., Goldman, A., Perevalov, V.I., Tashun, S.A., Tennyson, J.. (2010). HITEMP, the high-temperature molecular spectroscopic database. *J. Quant. Spectrosc. Radiat. Transf.*, 111, 2139–2150.

[56] Wójcik, W., Cięszczyk, S., Golec, T. (2010). Narrow-band spectra models for diagnostic of gases produced during the biomass production. L. Pawłowski, M. Dudzińska, A. Pawłowski (eds.). *Environmental Engineering* III, CRC Press, 597–601.